Materials Research Express

High thermoelectric power factor in $SnSe_2$ thin film grown on Al_2O_3 substrate

To cite this article before publication: Anh-Tuan Duong *et al* 2019 *Mater. Res. Express* in press https://doi.org/10.1088/2053-1591/ab1031

High thermoelectric power factor in $SnSe_2$ thin film grown on Al_2O_3 substrate

Anh Tuan Duong[1,2*], Dinh Lam Nguyen[3], Manh Nghia Nguyen[4], Thi Minh Hai Nguyen[5], Anh Duc Nguyen[5], Anh Tuan Pham[5], Parman Ullah[5], Zeeshan Tahir[5], Yong Soo Kim[5], Do Quang Trung[1,2], Tu Nguyen[1,2], Hao Van Bui[1,2], Raja Das[1,2], Pham Thanh Huy[1,2], and Sunglae Cho[5*]

[1] *Phenikaa Institute for Advanced Study, Phenikaa University, Yen Nghia, Ha-Dong district, Hanoi 10000, Vietnam*

[2]*Phenikaa Research and Technology Institute, A&A Green Phoenix Group, 167 Hoang Ngan, Hanoi 10000, Vietnam*

[3]*Department of Science in Engineering Physics, University of Engineering and Technology, Vietnam National University, Hanoi 10000, Vietnam*

[4]*Department of Physics Hanoi National University of Education, Hanoi 10000, Vietnam*

[5]*Department of Physics and Energy Harvest-Storage Research Center, University of Ulsan, Ulsan 680-749, Republic of Korea.*

Abstract

Thermoelectric figure of merit (ZT) is highly sensitive to the carrier concentration and maximizes within the narrow region of 10^{19} – 10^{20} cm^{-3}. The $SnSe_2$ single crystal is predicted to have a high ZT value with carrier concentration in the range of 10^{19} – 10^{20} cm^{-3}. Here, we grew $SnSe_2$ thin film on Al_2O_3 substrate by Pulsed Laser Deposition (PLD) with post annealing at 400 ^oC in Argon for 60 min. The annealed thin film shows a high thermoelectric power factor up to 8 $\mu Wcm^{-1}K^{-2}$ at 220 K with a carrier concentration of 5.2×10^{19} cm^{-3}. A hexagonal crystal structure of the $SnSe_2$ thin film was confirmed by x-ray diffraction and Raman spectra measurements. The thin film showed an n-type semiconductor behavior. Maximum electrical conductivity and Seebeck coefficient were obtained at 220 K with the values of 210 $S.cm^{-1}$ and -192 μVK^{-1}, respectively.

Corresponding authors: Dr. Anh-Tuan Duong Email: tuan.duonganh@phenikaa-uni.edu.vn

Prof. Sunglae Cho Email: slcho@ulsan.ac.kr

1. Introduction

Thermoelectric materials have been attracted the interest of researchers as it directly converts heat energy (including the wasted energy of heat) to electrical energy, and vice versa. A thermoelectric material is evaluated by the thermoelectric figure of merit ($ZT = S^2\sigma T/\kappa$) value, where S, σ, κ and T represent the Seebeck coefficient, electrical conductivity, thermal conductivity, and absolute temperature, respectively. [1,2] To increase ZT value, thermoelectric power factor, which is defined as the $PF = S^2\sigma$ should be maximized and thermal conductivity (κ) should be minimized. Thermoelectric power factor can be enhanced through the optimized carrier concentration, energy filtering of charge carriers, or increase the mobility (μ) of the charge carrier while thermal conductivity can be reduced by adding the number of interfaces and phonon scattering centers in nanostructure such as nanowire, nanotube, superlattice, or nanocomposite.[3–6] In recent years, the devices for local cooling and micro-thermoelectric power generation devices, which have been used Peltier and Seebeck effects in thermoelectric thin films are attracting the interest of electronic manufacturers for applications in the mobile and wireless devices. Therefore, many research groups have been trying to enhance the thermoelectric performance of thin films. For examples, A. Hmood *et al.* observed high thermoelectric power factors up to 45.25 μW cm^{-1} K^{-2} in the $Pb_{0.925}Yb_{0.075}Se_{0.2}Te_{0.8}$ and 31.3 μW cm^{-1} K^{-2} in the $Sn_{0.9}Yb_{0.1}Te$ thin films, and 18.7 μW cm^{-1} K^{-2} in the $AgPb_8SbTe_{10}$ sample. [7–9] Phuoc-Huu Le *et al.* observed a high thermoelectric power factor of 24.3 μW cm^{-1} K^{-2} in the Bi_2Te_3 thin film on SiO_2/Si (100) substrate.[10] By doping Pb into Bi_2Te_3, Yang Zhou et al. obtained power factor up to 25 μW cm^{-1} K^{-2} at 473 K.[11] H. Chang et al. achieved the maximum power factor of 12.4 μW cm^{-1} K^{-2} by annealing Sb_2Te_3 thin film at 220 °C for 60 min.[12] By using the p-type $Sn_{0.9}Yb_{0.1}Te$:Te and n-type $Sn_{0.9}Yb_{0.1}Te$, A. Hmood *et al.* fabricated the micro-thermoelectric device with the maximum open-circuit voltage output of 823.7 mV and a maximum output power of 0.259 μW at a temperature difference of 180 K and the hot-side temperature (T_h) of 528 K.[13]

Among the layer structure semiconductors family, SnSe and $SnSe_2$ were predicted as the good materials for thermoelectric applications due to their ultra-low thermal conductivity. Experimental results showed that ZT values of the orthorhombic SnSe single crystal can be achieved to 2.6 at 933 K for p-type SnSe and 2.2 at 733 K for n-type with doping of Bi

while theoretical calculation predicted that ZT value of $SnSe_2$ single crystal can be achieved up to 2.95 with the carrier concentration of 10^{20} cm^{-3}.[14–16] $SnSe_2$ has a hexagonal crystal structure of the type CdI2 with $P\bar{3}m1$ space group, which is characterized by a van der Waals bonding force between Sn-Se-Sn layers along the c-axis direction. Lattice parameters of hexagonal $SnSe_2$ are a = b = 3.811 Å and c = 6.141 Å.[17] $SnSe_2$ has been identified as an n-type semiconductor with an indirect band gap of 0.97 eV.[18] Recently, several research groups have been focused on the enhancement of thermoelectric performance of bulk $SnSe_2$ and achieved some promising results. By doping Cl, Peipei Xu *et al.* obtained maximum PF of 7.0 $\mu W\ cm^{-1}\ K^{-2}$ and ZT value of 0.4 in the 6% of Cl substituting in $SnSe_2$ polycrystalline. [19] Fu Li *et al.* obtained the highest PF of 4 $\mu W\ cm^{-1}\ K^{-2}$ and ZT value of 0.4 in the $Sn_{0.99}Ag_{0.01}Se_2$.[20], Yixuan Wu *et al.* enhanced ZT of $SnSe_2$ up to 0.6 at 750 K by substituting Br into Se sites of $SnSe_2$.[21] $(SnSe_2)_{0.67}(Bi_2Se_3)_{0.33}$ compound has PF = 3.1 $\mu W\ cm^{-1}\ K^{-2}$.[22] Additionally, other properties such as electrical transport and optical properties of $SnSe_2$ were also studied.[23–28] For $SnSe_2$ thin films, most of the reports focused on characteristic structure, electrical, and optical properties.[29–33] Some groups have reported on the growth condition of $SnSe_2$ thin films. [34–36] To best of our knowledge, there has been no study about thermoelectric properties of the $SnSe_2$ thin film. This article introduces a study on thermoelectric properties of the $SnSe_2$ on Al_2O_3 substrate in which the power factor value can be achieved up to 8 $\mu Wcm^{-1}K^{-2}$ at 220 K.

2. Experiment

$SnSe_2$ thin films were grown on an Al_2O_3 substrate by Pulsed Laser Deposition (PLD) method from a $SnSe_2$ single crystal target. The $SnSe_2$ target was fabricated from high purity (5N) of Sn and Se powder by temperature gradient method under following process. After loading materials inside, the quartz ampoule was sealed under vacuum (> 10^{-3} Torr). Materials in quartz ampoule was slowly heated to 750 ^oC and maintained at this temperature for 10 h. Finally, it was slowly cooled down to room temperature. Obtained $SnSe_2$ single crystal with the dimension of 14 mm was used as a target for PLD growth. Al_2O_3 substrate was chemically cleaned by methanol before being loaded into the growth chamber. A krypton fluoride (KrF) excimer laser (λ = 248 nm, CompexPro 102F) with 20 ns pulse width was used for deposition of $SnSe_2$ thin film. The thin film was deposited by

pulsed of laser repetition rate of 3 Hz in 20 min under a base pressure of 10^{-4} Torr and the substrate temperature of 100 ^{o}C. Haft of $SnSe_2$ thin film was annealed in Argon gas at 400 ^{o}C for 60 min. The crystal structure of the thin film was characterized by X-ray diffraction [model D/max-RC, Rigaku Co., Tokyo, Japan]. Surface morphology was characterized by a field emission scanning electron microscope (FE-SEM). Physical property measurement system (PPMS) was used to characterize the electrical resistivity, the Seebeck coefficient, and the Hall resistance.

3. Results and Discussions

The crystal structure of $SnSe_2$ bulk (as the target) and thin film were confirmed by XRD patterns as shown in Fig. 1 (a). The locations of diffraction peaks of both target and film indicated a single phase - hexagonal structure of $SnSe_2$. Only *(00l)* diffraction peak group indicated that $SnSe_2$ single crystal was successfully fabricated by the gradient temperature method. Two diffraction peak groups of *(00l)* and *(h0l)* appeared in the $SnSe_2$ thin film corresponding a polycrystalline nature. By using Bragg's Law, interplanar distance d_{001} (*c* lattice constant) of the $SnSe_2$ thin film was determined to be 6.173 Å. It is a little larger than that of $SnSe_2$ bulk. An in plane compress strain due to the lattice mismatch between Al_2O_3 substrate and $SnSe_2$ thin film may be the cause of the increase the *c* lattice constant and the shift of XRD peaks. Fig. 1 (b) shows the Raman spectrum from 100 to 300 cm^{-1} at room temperature for the $SnSe_2$ thin film. Two Raman vibration modes E_g and A_{1g} appear at 119.1 cm^{-1} and 185.7 cm^{-1} are characteristic of the hexagonal $SnSe_2$ phase. Surface morphologies of cleaved $SnSe_2$ bulk crystal and thin film were observed by FE-SEM images as shown in Fig. 2. A lamellar microstructure with few μm of average thickness was observed in the cleaved bulk target while the surface of the $SnSe_2$ thin film is relatively uniform. The thickness of the thin film as shown in the inset of Fig. 2 (b) is 85 nm.

Hall resistance, which is a function of an external magnetic field at the selected temperature and temperature dependent carrier concentration from 50 to 400 K of $SnSe_2$ thin film, are shown in Fig. 3. The negative slopes of a Hall resistance indicated an existence of an n-type semiconductor behavior in the $SnSe_2$ thin film. From the slope of V_H/I against the magnetic field, the carrier concentrations of the $SnSe_2$ thin film was calculated using the formula, $\frac{V_H}{I} = \frac{1}{ned}H$, where V_H is the Hall voltage, *I* is the electrical current, n is the number of carriers, *e* is the electrical charge, H is the magnetic field, and d is the thickness of thin

film. Carrier concentration increases from 4.8×10^{19} to 6.2×10^{19} cm^{-3} with an increment of temperature from 50 to 400 K. As the prediction of theoretical calculations, this region carrier concentration is a good sign for thermoelectric properties of $SnSe_2$.[16,37]

The temperature-dependent electrical conductivity of the $SnSe_2$ thin film is shown in Fig. 4 (a). The $SnSe_2$ thin film exhibited semiconductor behavior in all temperature range. The electrical conductivity increase with increasing temperature from low temperature to 220 K. But at the temperature higher than 220 K the decrease of electrical conductivity may due to the competing factor of carrier concentration (n) and carrier mobility (μ).[7] Maximum electrical conductivity is 212.7 $S.cm^{-1}$ at 220 K, comparable to some experimental results in the bulk $SnSe_2$ crystal with the Cl or Br doping[19,21] and similar to the theoretical calculation result at the same carrier concentration order of D. Yingchun et al.[16] The enhancement of carrier concentrations is the cause of high electrical conductivity in the annealed $SnSe_2$ thin film. A similar trend with electrical conductivity was observed in the temperature dependent Seebeck coefficient as shown in Fig. 4 (b). The negative Seebeck coefficient confirmed for n-type semiconductor behavior of the sample. The value of the Seebeck coefficient sharply increases from low temperature until 220 K with a maximum value of - 192 μVK^{-1} and slowly reduce with higher temperature. The different of Seebeck coefficient between below and above 220 K also attributed for the competing of carrier concentration and carrier mobility.

Thermoelectric power factor (PF), which is an important parameter of thermoelectric materials is determined from electrical conductivity and Seebeck coefficient results as shown in Fig. 5. Highest Power factor value of annealing $SnSe_2$ thin film is 8 $\mu Wcm^{-1}K^{-2}$ at 220 K. Comparable to experimental results of pure $SnSe_2$ bulk crystalline, PF of annealing $SnSe_2$ thin film is greatly improved.

4. Conclusion

The high thermoelectric power factor is obtained in a hexagonal structure $SnSe_2$ thin film grown on Al_2O_3 substrate. By annealing effects, we can achieve carrier concentration order in region of $10^{19} - 10^{20}$ cm^{-3}, which is the best value for thermoelectric performance. Electrical conductivity increased significantly in thin films compared to that of bulk samples. The high thermoelectric power factor of 8 $\mu Wcm^{-1}K^{-2}$ can be attributed to that the high electrical conductivity due to annealing while maintaining a high Seebeck

coefficient. With a high-power factor value, $SnSe_2$ thin film is a promising material for thermoelectric micro-devices.

This research is funded by Vietnam National Foundation for Science and Technology Development (NAFOSTED) under grant number 103.02-2016.09

References

[1] Tritt T M and Subramanian M a 2006 Thermoelectric Materials, Phenomena, and Applications : A Bird' s Eye View *MRS Bull.* **31** 188–98

[2] Gaultois M W, Sparks T D, Borg C K H, Seshadri R, Bonificio W D and Clarke D R 2013 Data-Driven Review of Thermoelectric Materials: Performance and Resource Considerations BT - Chemistry of Materials *Chem. Mater.* **25** 2911–20

[3] Paul B and Banerji P 2009 Grain Structure Induced Thermoelectric Properties in PbTe Nanocomposites *Nanosci. Nanotechnol. Lett.* **1** 208–12

[4] Heremans J P, Jovovic V, Toberer E S, Saramat A, Kurosaki K, Charoenphakdee A, Yamanaka S and Snyder G J 2008 Enhancement of Thermoelectric of the Electronic Density of States *Science (80-.).* **321** 554–7

[5] Goldsmid H J 2012 Impurity Band Effects in Thermoelectric Materials *J. Electron. Mater. August* **41** 2126–9

[6] Yu B, Zebarjadi M, Wang H, Lukas K, Wang H, Wang D, Opeil C, Dresselhaus M, Chen G and Ren Z 2012 Enhancement of Thermoelectric Properties by Modulation-Doping in Silicon Germanium Alloy Nanocomposites *Nano Lett.* **12** 2077–82

[7] Hmood A, Kadhim A and Hassam H A 2014 Superlattices and Microstructures Yb-doped SnTe semimetal thin films deposited by thermal evaporation : Structural , electrical , and thermoelectric properties *SUPERLATTICES Microstruct.* **76** 36–45

[8] Hmood A, Kadhim A and Hassan H A 2012 Enhancement of electrical transport through the anisotropic nanostructure performance of heavily Yb-doped PbSe 0 . 2 Te 0 . 8 thin fi lms *Mater. Chem. Phys.* **136** 1148–55

[9] Hmood A, Kadhim A, Mahdi M A and Hassan H A 2016 ScienceDirect Structural

, characterization and electrical properties of AgPb m SbTe m þ 2 compounds synthesized through a solid-state microwave technique *Int. J. Hydrogen Energy* **41** 5048–56

[10] Le P H, Liao C N, Luo C W and Leu J 2014 Thermoelectric properties of nanostructured bismuth-telluride thin films grown using pulsed laser deposition *J. Alloys Compd.* **615** 546–52

[11] Zhou Y, Li L, Tan Q and Li J F 2014 Thermoelectric properties of Pb-doped bismuth telluride thin films deposited by magnetron sputtering *J. Alloys Compd.* **590** 362–7

[12] Chang H, Kao M-J, Peng C-H, Kuo C-G and Huang K-D 2011 Thermoelectric Properties of Sb2Te3 Thin Films by Electron Beam Evaporation *J. Nanosci. Nanotechnol.* **11** 7491–4

[13] Hmood A, Kadhim A and Hassan H A 2018 Thin-film thermoelectric device of semimetals p-Sn0.9Yb0.1Te:Te and n-Sn0.9Yb0.1Te for power generation using thermal evaporation *Measurement* 0–27

[14] Zhao L-D, Lo S-H, Zhang Y, Sun H, Tan G, Uher C, Wolverton C, Dravid V P and Kanatzidis M G 2014 Ultralow thermal conductivity and high thermoelectric figure of merit in SnSe crystals *Nature* **508** 373–7

[15] Duong A T, Nguyen V Q, Duvjir G, Duong V T, Kwon S, Song J Y, Lee J K, Lee J E, Park S, Min T, Lee J, Kim J and Cho S 2016 Achieving ZT=2.2 with Bi-doped n-type SnSe single crystals *Nat. Commun.* **7** 1–6

[16] Ding Y, Xiao B, Tang G and Hong J 2017 Transport properties and high thermopower of SnSe2: A full ab-initio investigation *J. Phys. Chem. C* **121** 225–36

[17] Julien C, Eddrief M, Samaras I and Balkanski M 1992 Optical and electrical characterizations of SnSe, SnS2 and SnSe2 single crystals *Mater. Sci. Eng. B* **15** 70–2

[18] Domingo G, Itoga R S and Kannewurf C R 1966 Fundamental Optical Absorption in SnS2 and SnSe *Phys. Rev.* **143** 536–41

[19] Xu P, Fu T, Xin J, Liu Y, Ying P, Zhao X, Pan H and Zhu T 2017 Anisotropic

thermoelectric properties of layered compound SnSe2 *Sci. Bull.* **62** 1663–8

[20] Li F, Zheng Z, Li Y, Wang W, Li J F, Li B, Zhong A, Luo J and Fan P 2017 Ag-doped SnSe2 as a promising mid-temperature thermoelectric material *J. Mater. Sci.* **52** 10506–16

[21] Wu Y, Li W, Faghaninia A, Chen Z, Li J, Zhang X, Gao B, Lin S, Zhou B, Jain A and Pei Y 2017 Promising thermoelectric performance in van der Waals layered SnSe 2 *Mater. Today Phys.* 1–10

[22] Kozma A A, Sabov M Y, Peresh E Y, Barchiy I E and Tsygyka V V. 2015 Thermoelectric properties of a eutectic SnSe2-Bi2Se3 alloy *Inorg. Mater.* **51** 93–7

[23] Lucovsky G, Mikkelsen J C J, Liang W Y, White R M and Martin R M 1976 Optical phonon anisotropies in the layer crystals Sn S 2 and Sn Se 2 *Phys. Rev. B* **14** 1663–9

[24] Borges Z V., Poffo C M, De Lima J C, De Souza S M, Trichês D M, Nogueira T P O, Manzato L and De Biasi R S 2016 Study of structural, optical and thermal properties of nanostructured SnSe2prepared by mechanical alloying *Mater. Chem. Phys.* **169** 47–54

[25] Wen S, Pan H and Zheng Y 2015 Electronic properties of tin dichalcogenide monolayers and effects of hydrogenation and tension *J. Mater. Chem. C* **3** 3714–21

[26] Huang Y, Chen X, Zhou D, Liu H, Wang C, Du J, Ning L and Wang S 2016 Stabilities, Electronic and Optical Properties of $SnSe_{2(1-x)}S_{2x}$ Alloys: A First-Principles Study *J. Phys. Chem. C* **120** 5839–47

[27] Saha S, Banik A and Biswas K 2016 Few-Layer Nanosheets of n-Type SnSe2 *Chem. - A Eur. J.* **22** 15634–8

[28] Yu P, Yu X, Lu W, Lin H, Sun L, Du K, Liu F, Fu W, Zeng Q, Shen Z, Jin C, Wang Q J and Liu Z 2016 Fast Photoresponse from 1T Tin Diselenide Atomic Layers *Adv. Funct. Mater.* **26** 137–45

[29] Mukhokosi E P, Krupanidhi S B and Nanda K K 2017 Band Gap Engineering of Hexagonal SnSe2 Nanostructured Thin Films for Infra-Red Photodetection *Sci. Rep.* **7** 15215

[30] Guillén C, Montero J and Herrero J 2011 Characteristics of SnSe and SnSe 2 thin films grown onto polycrystalline SnO2-coated glass substrates *Phys. Status Solidi Appl. Mater. Sci.* **208** 679–83

[31] Tracy B D, Li X, Liu X, Furdyna J, Dobrowolska M and Smith D J 2016 Characterization of structural defects in SnSe2thin films grown by molecular beam epitaxy on GaAs (111)B substrates *J. Cryst. Growth* **453** 58–64

[32] Hady D A, Soliman H, El-Shazly A and Mahmoud M S 1999 Electrical properties of SnSe2 thin films *Vacuum* **52** 375–81

[33] Saritha K, Suryanarayana Reddy A and Ramakrishna Reddy K T 2017 Investigation on Optical Properties of SnSe2Thin Films Synthesized by Two - Stage Process *Mater. Today Proc.* **4** 12512–7

[34] Tracy B D, Liu X, Furdyna J K and Smith D J 2016 Thin Films of SnSe 2 Grown by Molecular Beam Epitaxy on GaAs (111)B Substrates *Microsc. Microanal.* **22** 1546–7

[35] Barrios-Salgado E, Nair M T S and Nair P K 2016 Thin films of n-type SnSe2produced from chemically deposited p-type SnSe *Thin Solid Films* **598** 149–55

[36] Boscher N D, Carmalt C J, Palgrave R G and Parkin I P 2008 Atmospheric pressure chemical vapour deposition of SnSe and SnSe2 thin films on glass *Thin Solid Films* **516** 4750–7

[37] Li G, Ding G and Gao G 2017 Thermoelectric properties of $SnSe_2$ monolayer *J. Phys. Condens. Matter* **29** 015001

Figure captions

Fig. 1. (color online) (a) Room temperature XRD patterns of bulk target $SnSe_2$ and annealed $SnSe_2$ thin film on Al_2O_3 substrate. (b) Room temperature Raman spectrum of annealed $SnSe_2$ thin films.

Fig. 2. (color online) FE-SEM images of (a) cleaved bulk target $SnSe_2$ and annealed $SnSe_2$ thin film. Inset of (b) is FE-SEM cross-section image for the determined thickness of thin film.

Fig. 3. (color online) (a) V_{Hall}/I versus magnetic field curves of annealed $SnSe_2$ thin film at the selected temperature, (b) Temperature-dependent carrier concentration of annealed $SnSe_2$ thin film.

Fig. 4. (color online) (a) Electrical conductivity as a function of temperature, (b) Temperature-dependent Seebeck coefficient of annealed $SnSe_2$ thin film.

Fig. 5. (color online) Temperature-dependent thermoelectric power factor of annealed $SnSe_2$ thin film.

Fig. 1

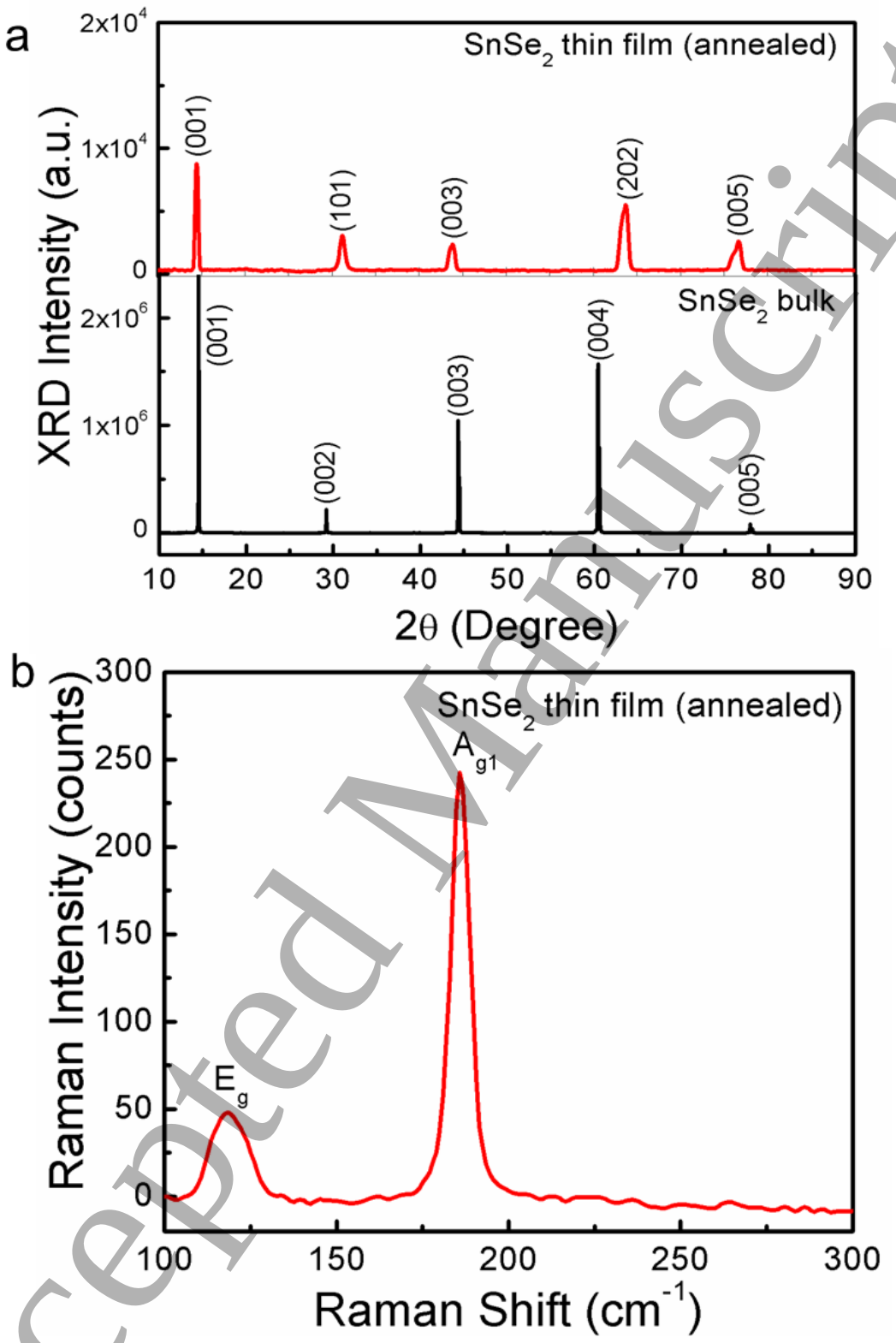

Fig. 2

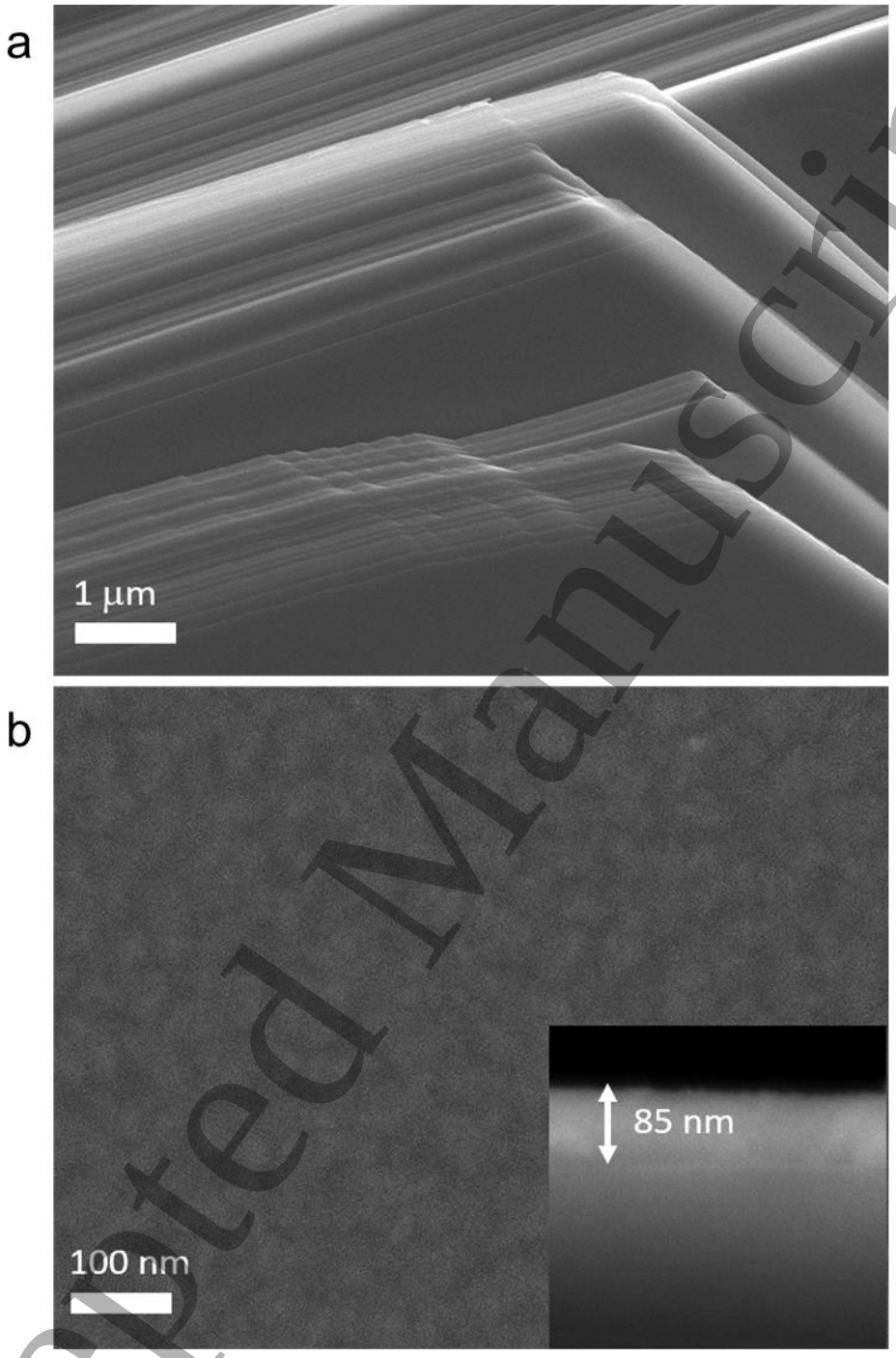

Fig. 3

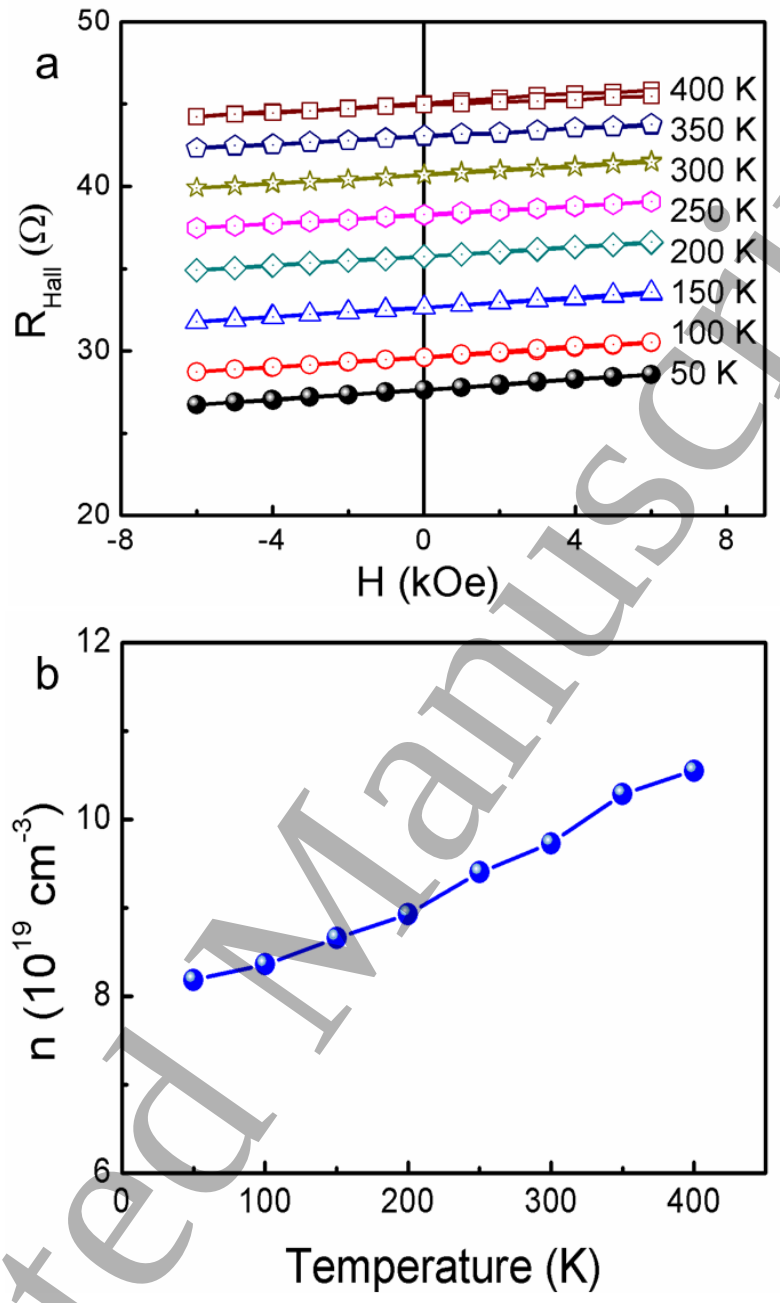

Fig. 4

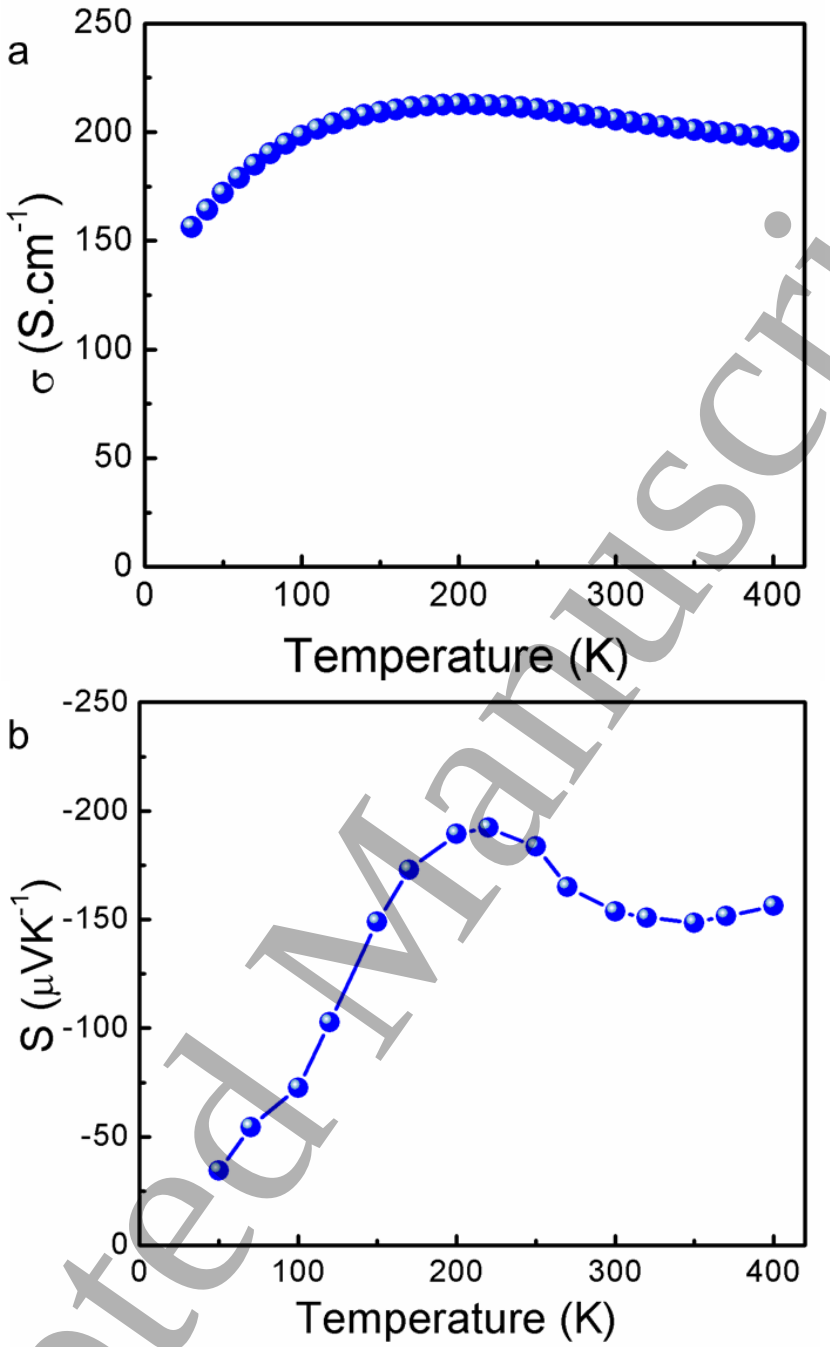

Fig. 5